Science World Journal Vol. 18(No 4) 2023 DOI: https://dx.doi.org/10.4314/swj.v18i4.2
www.scienceworldjournal.org
ISSN: 1597-6343 (Online), ISSN: 2756-391X (Print)
Published by Faculty of Science, Kaduna State University

Full Length Research Article

INVESTIGATION INTO A DEEP-ROOTED CRUSTAL FRAMEWORK DEDUCED FROM POTENTIAL FIELD DATA IN CRETACEOUS AND TERTIARY STRATA, SOKOTO BASIN NW, NIGERIA

*[1]Adamu Abubakar, [2]Othniel Kamfani Likkason, [3]Abdulganiyu Yunusa, [1]Hadiza Umar Tsafe, [4]Umar Mahmood, [4]Bala Balarabe and [5]Andarawus Yohanna

[1]Department of Applied Geophysics, Federal University Birnin Kebbi, P.M.B. 1157, Kebbi State, Nigeria
[2]Department of Physics, Abubakar Tafawa Balewa University Bauchi, P.M.B. 1051, Bauchi State, Nigeria
[3]Department of Geology, Federal University Birnin Kebbi, P.M.B. 1157, Kebbi State, Nigeria
[4]Department of Physics, Ahmadu Bello University Zaria, P.M.B. 1049, Zaria, Nigeria
[5]Department of Geology, Federal University of Lafia, Nasarawa State, Nigeria

*Corresponding Author Email Address: adamu.abubakar35@fubk.edu.ng

ABSTRACT
The Paleocene sediments from the Sokoto Group, which comprises of the Gamba, Dange, and Kalambaina formations, were covered by Maastrichtian sediments from the Rima Group, which includes the Wurno, Dukamaje, and Taloka formations. High-resolution aeromagnetic and satellite gravity measurements were used to study these sediments. The aforementioned strata correspond to the Cretaceous and Tertiary strata in this research area and are situated in the south-eastern part of the Iullemmeden Basin. Our aim is to determine and explain the horizontal variation in density and magnetization using the whole regional satellite gravity and aeromagnetic data. The deeper magnetic and density sources were scanned using a two-dimensional (2D) radially averaged power spectrum analysis to produce the NE to SW and E to W trending models for the Moho, lower, and upper lithosphere under the study area. The results were further assessed using upward continuation, derivative analysis, and two-dimensional gravity and magnetic modeling. Numerous important structural trends (i.e., NE-SW, E-W & ENE-WSW), have been identified as a result of the vertical gradients for the potential field data. Spectral analysis and Euler deconvolution can be used to calculate the depths to the lower and upper mantle crust boundaries as well as the depth to Moho**.** The findings of a qualitative analysis point to an intrusion of the Gundumi and Illo Formations that has a northeast orientation as the primary cause of the significant gravitational and magnetic interaction. The differences in the deep-seated crustal structures and mineralized anomalous bodies with depth were visible on anomaly maps with an upward continuation of 5 km, 7 km, 20 km, and 30 km. Quantitatively, the 2D regional models along the selected profiles (L_1, L_2, L_4, L_6 and L_7) display a typical lithostratigraphic succession of the Gundumi and Illo Formation (Continental Intercalaire, CI) type of crust, which is subdivided into the lower and upper mantle crust as well as the Moho. The sediment thickness by surface depth ranges from ~4.06 km and ~23.31 km. The Moho interface, lower and upper mantle crusts, and magnetic crust are all located at depths of around ~10.23 km. The distance between the local models of the foundation rocks to the north and south of the Sokoto Group was approximately ~6 to ~8 km and ~4.5 km, respectively.

Keywords: aeromagnetic data; satellite gravity data; Crustal framework; Cretaceous and Tertiary strata; Enhancement filtering techniques; 2D forward modeling.

INTRODUCTION
The West and Central African Rift Systems (WCARS), also known as the Cretaceous Rift Systems of West and Central Africa, are made up primarily of the Cretaceous-Paleocene rifts in the Central African Republic, Niger, and Chad. They span about 4000 km from Nigeria northward into Niger and Libya and eastward through southern Chad into Sudan and Kenya. According to Darly et al. (1989), the Pan-African zone of lithospheric weakness includes the Cretaceous rifts. The Central African Rift Subsystem (CAS) and the Western African Rift Subsystem (WAS) are the two coeval Cretaceous rift subsystems that make up this rift system zone. Each of the subsystems contains a set of strike-slip fractures that extend deeply into the African continent (Fairhead, 1992).
The Sokoto inland basin is now being assessed within the context of a tectonic and geodynamic setting, because it is an essential component in understanding the origin of the West and Central African Rift System (WCARS) (Obaje, 2009). Because most geologic activities are not only hidden from human direct observation but also highly slow-moving processes that do not complete over the lifespan of people, it can be difficult to understand the geodynamic setting of a region. Gravity data analysis is used to evaluate density distribution, which confirms the findings of geophysical, geological, and geodetic evidence. Examining deep and shallow crustal features can show a deep-rooted crustal framework; these crustal phenomena can be identified using geophysical survey techniques. Deeper zones of crustal framework can now be studied using a common methodology that combines satellite gravity and aeromagnetic geophysical data (e.g. Sultan et al., 2009; Mekkawi, 2012; El-Galladi et al., 2016, Mousa et al., 2020; Araffa et al., 2020; Mekkawi et al., 2021; Salem et al., 2011; Alexander et al, 2015; Ghazala et al., 2016, El-dosouky et al., 2017; Gabr et al., 2022). For purposes involving the deep crustal framework, measurements of a variety of Earth's surface and subsurface characteristics are necessary, e.g., geologic structures, lithologic and mineral resources, mapping geology, faults, and fractures (Adamu and Likkason, 2022; Adamu et al., 2020). Satellite gravity data was used to create an image of the likely position and magnitude of zones that may contain melt and mafic dykes in the lower crust. Various potential field data, including satellite gravity and aeromagnetic data, are efficiently integrated to determine the depth of the boundary between the upper and lower crust and to delineate regional and local structures using two-dimensional (2D) radially-average power spectra (hereinafter referred to as spectral analysis). Satellite gravity data draw attention to lithologic contacts which are

Science World Journal Vol. 18(No 4) 2023 DOI: https://dx.doi.org/10.4314/swj.v18i4.2
www.scienceworldjournal.org
ISSN: 1597-6343 (Online), ISSN: 2756-391X (Print)
Published by Faculty of Science, Kaduna State University

most likely situated around crustal structures, where these contacts would have indicated a Crustal extension. The Sokoto Basin's shallow and deep geologic frameworks were mapped, and the depth of the magnetic boundary between Cretaceous and Tertiary formations was revealed through the analysis and enhancement of aeromagnetic and satellite gravity data. These crustal events are reflected in the trends and intensities shown on aeromagnetic maps that show magnetic patterns. The texture analysis also made it possible to improve and identify geologic lineaments such as joints, faults, and lithologic boundaries. Over the past few decades, a number of studies have concentrated on characterizing the structure of magnetic field data (Likkason, 2014; Likkason et al. 2013; Likkason, 2011; Adamu et al. 2022; Bonde et al. 2014; Nwankwo and Shehu, 2015).This is due to the fact that tectonic activity in nature appears as a nearly round shape, and is linked to the crustal framework. These continental crusts were frequently surrounded by structural features that showed subsequent or concentrated zones (Kogbe, 1979). As a result, several studies concentrated on using aeromagnetic data to identify the structural features. Many studies have been conducted in the area, such as Adamu et al. (2022) who described the regional patterns and imaged the upper lithospheric structures and its Hydrocarbon implication from Gwandu formation northwestern Nigeria. Using the first regionally extensive satellite gravity and aeromagnetic data, our aim is to understand and provide an explanation for the lateral differences in density and magnetization across the entire formations in the Sokoto Basin. This entails in calculating the separation between Cretaceous and Tertiary formations, the depth between the upper and lower mantle crustal borders, and the depth to the Moho. The satellite gravity and aeromagnetic data were integrated to produce a two-dimensional (2D) model with a NW to SE and E to W trend in order to image the deeper magnetic and density sources in the study area.

STUDY AREA: LOCATION AND ITS GEOLOGICAL SETTINGS

In northwestern Nigeria, between latitudes 10° 20′ and 12° 00′ N and longitudes 4° 00′ and 5° 00′ E, the Sokoto basin occupies about 6.4 x 10^4 km^2 of land (Fig 1). It's located in an area where there is an erratic distribution of rainfall in terms of time and place, with a protracted dry season and a brief wet season. A moderated undulating plain with an average elevation from 250 to 400 meters above sea level makes up a majority of the Sokoto sedimentary basin in northwestern Nigeria. The monotous plain is occasionally broken up by flat-topped, steep-sided hills, with "Dange Scarp" being the most noticeable feature in the basin, according to Kogbe (1979). The "Dange Scarp" has been extensively eroded to the point where it's no longer discernible due to the escarpment intimate relationship to the local geology of the region (Udoh, 1970). As a part of the Sub-Saharan Sudan belt of West Africa, the climate is semi-arid with a region of savannah-type flora. The Sokoto Basin experiences significant variations in rainfall, with annual mean precipitation ranging from 350 mm (near Kalmalo in the far north) to 670 mm (at the Sokoto, Argungu). When compared to the dry season, which lasts for more than 5 months without a single raindrop, the short wet season which lasts from mid-May to mid-September has a high concentration of rainfall. The range of the average annual temperature is 21.5 to 34.9°C. The months with the highest temperatures are April through July, while August has the lowest (during the rainy season) (Udoh, 1970). The sediments of the Sokoto Basin in northwestern Nigeria were accumulated three distinct time periods: the Continental Mesozoic and Tertiary periods, with an interstitial marine Maastrichtian to Paleocene. The Sokoto Basin's sedimentary sequence is depicted in Table 1. The Illo and Gundumi Formations, which are composed of grits and clays and are a parts of West Africa's "Continental" intercalair, overlie the Precambrian basement in an irregular manner (Kogbe, 1981). These are separated by the fossiliferous shaly Dukamaje Formation and overlain irregularly by the Maastrichtian Rima group, which is composed of mudstones and friable sandstones (Taloka and Wurno Formations). The calcareous Kalambaina formation divides the Paleocene Dange Formation, which is primarily composed of shales. Tertiary in age is the underlying continental Gwandu Formation (Continental Terminal) (Jones, 1948; Kogbe, 1981). Near the border with the Niger Republic, these sediments have a maximum thickness of nearly 1,200 meters and dip gently before gradually thickening in northwest (Wright et al., 1985; Kogbe, 198).

The topography and surface elevations of the several rock units in the area of study are used to create the 30 m accurate ASTER Global Digital Elevation Model (GDEM). Elevations vary between 250 to 400 meters above sea level (asl) (Fig. 2a). The territory to the north, south, and east is defined by positive topography. To the southwest, where all formations are merging at Gwandu to drain in Quaternary alluvium, moderate to low heights can be seen (Fig. 2a). The direct correlation between altitudes and various lithological units, which may be utilized to pinpoint rock units and determine the crustal framework over the Sokoto Basin, is the most intriguing geomorphological point. For instance, the highest topographies reflect the late-to-post tectonic Gundumi/Illo formations (made of grits and clays and a portion of West Africa's "Continental" intercalair to the northeast corner), which range in altitude from 350 to 695 m. the fossiliferous layers of the Rima group, which are found in the (Shaly Dukamaje, Taloka, and Wurno formations), 202 -250 m above mean sea level, asl. With the exception of the 120 – 202 m asl (Quaternary alluvium deposits that fill the Gwandu and Kalambaina Formations, all other rock groups are higher than metasediments. Additionally, slightly indurated bluish-grey shales limestone with bands of fibrous gypsum and irregular phosphatic nodules interbedded with thin layers of yellowish- brown limestone are simple to distinguish visually from surrounding rocks because they exhibit extremely raised, longitudinal and sharp ridges (Fig. 2b,c). In addition, the structural characteristics of ferruginous rocks, particularly laterite and kaolinitic clay, reveal extremely raised ridges in Duku-Tarasa and Gulma. Positive materials heights are correlated with their resistance to weathering. When compared to altered Basal conglomerates, gravel, sand, pisolithic and nodular clays, poorly fossiliferous to the north of the Gundumi/Illo formations of Continental Intercalair display higher relief in the Basal conglomerates of the Bagudo area. A few chosen profiles show connection between the heights of rock units and the occurrences of alteration to the right of Figure 2 b,c.

Science World Journal Vol. 18(No 4) 2023 DOI: https://dx.doi.org/10.4314/swj.v18i4.2
www.scienceworldjournal.org
ISSN: 1597-6343 (Online), ISSN: 2756-391X (Print)
Published by Faculty of Science, Kaduna State University

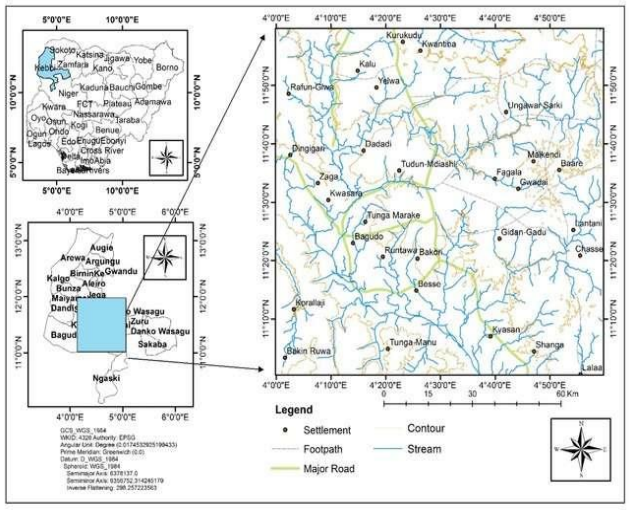

Figure 1: Location map of the Study Area (Adopted from Arc-GIS, 2019)

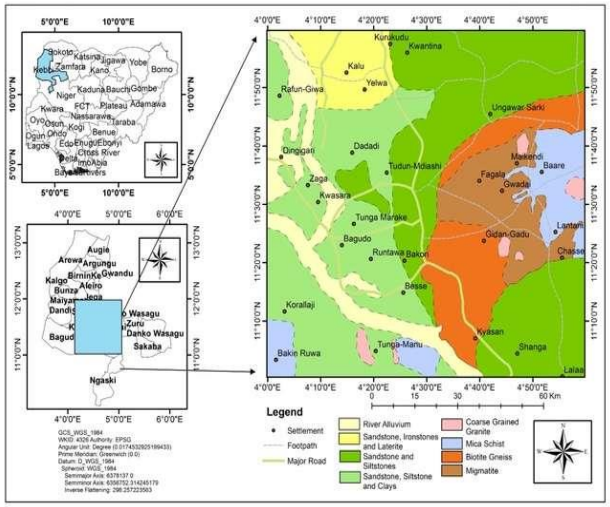

(a)

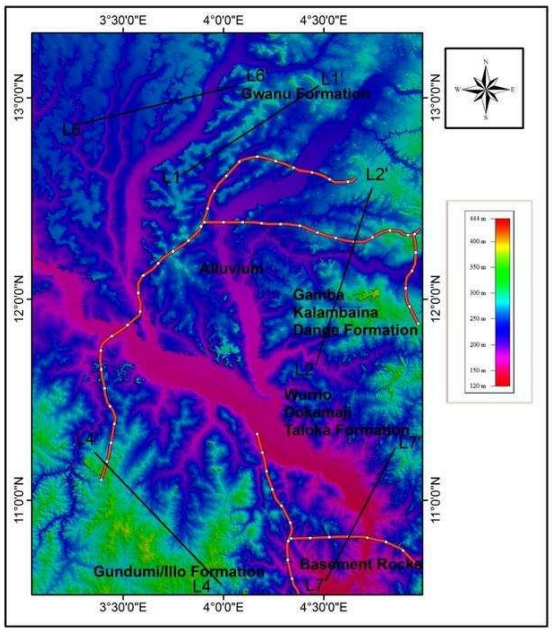

(b)

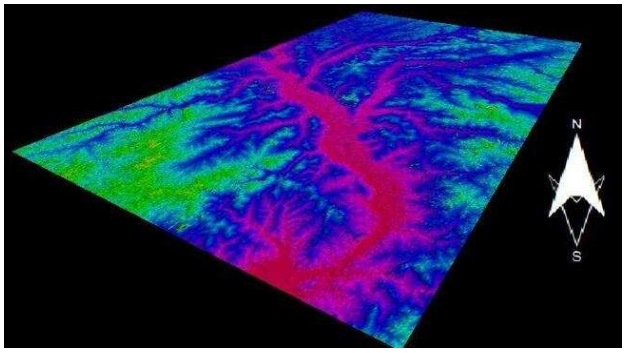

(c)

Figure 2: (a) Geological map of "Sub-Sokoto" Basin (b) shows a topographic map of the research area, based on ASTER GDEM (V3) and (c) a 3D topographic scene of the region

Cretaceous Rocks

The majority of the rocks from the Cretaceous period are sandstone and siltstone, with minor amounts of conglomerate, shale, mudstones, and ferruginous particles. These rocks show various marine transgressions and regressions and were primarily deposited in shallow water. They total about 13,000 feet in thickness overall. The Cretaceous rocks are distinguished from overlying younger rocks by a modest angular discordance and from the older rocks beneath by a noticeable angular unconformity (Kogbe, 1981). These locally highly fossiliferous Cretaceous rocks, which are also well exposed and only mildly deformed, serve as an important bio-stratigraphic reference section for strata that range in age from the Maastrichtian to the late Cenonian. The southern portions of the Taloka formation, the Gundumi/Illo formation, and the Dukamaje formation are all underlain by the Cretaceous rocks that are subject of this study (Kogbe, 1981; Jones, 1948). Many of the gently rolling hills bordering the 'Dutsen Tuta' range up to an altitude of 6,000 feet have these rocks growing out of them, which deeply incised the river Niger tributary (Fig. 2 b,c).

Science World Journal Vol. 18(No 4) 2023 DOI: https://dx.doi.org/10.4314/swj.v18i4.2
www.scienceworldjournal.org
ISSN: 1597-6343 (Online), ISSN: 2756-391X (Print)
Published by Faculty of Science, Kaduna State University

Table 1: Summary of Geological sequence of "Sokoto Basin", Northwestern, Nigeria after, (Jones, 1948; Kogbe, 1979)

AGE	FORMATION	DESCRIPTION	GROUP	ENVIRONMENT
(a) EOCENE-MIOCENE	GWANDU	Red mottled massive clays with sandstone intercalation and ironstone.	CONTINENTAL TERMINALE	Continental (Kogbe, 1972)
(b) PALEOCENE Montian-Landenian	GAMBA	Grey laminated shales with abundant fossil.	SOKOTO GROUP (Abduganiyu, 2021)	Marine (Kogbe, 1989)
	KALAMBAINA Calcareous Group (Kogbe, 1979)	White clayey limestones and shales with abundant fossil. Forams, Ostracods, Mollusks, Bivalves and Echinoids		
	DANGE (Kogbe, 1979) Clay-shale Group	Slightly indurated bluish-grey shales limestone with bands of fibrous gypsum and irregular phosphatic nodules interbedded with thin layers of yellowish- brown limestone.		
(c)MAASTRICHTIAN Upper Senonian, (Jones, 1948)	WURNO Upper Sandstones and Mudstones (Kogbe, 1979)	Pale friable fine-grained sandstone and siltstone with thin intercalated mudstone and carbonaceous mudstone with iron sulphide.	RIMA GROUP (Abduganiyu, 2021)	Continental (Kogbe, 1989).
	DUKAMAJE (Kogbe, 1979) Mosasaurus shales	Shales with some limestone, mudstone and gypsiferous shales with a bone bed which is an excellent marker horizon. It is highly fossiliferous.		Marine (Kogbe, 1989).
	TALOKA Lower Sandstones and Mudstones (Kogbe, 1979)	Friable white fine-grained sandstone and siltstone with thin intercalated mudstone and carbonaceous mudstone or shales containing gypsum and ferruginous particles.		Continental (Kogbe, 1989).
(d)PRE-MAASTRICHTIAN	GUNDUMI	Basal conglomerates, gravel, sand, pisolithic and nodular clays. Poorly fossiliferous.	CONTINENTAL INTERCALAIRE	Fluviatile and Lacustrine (Abduganiyu, 2021; Kogbe, 1979)
	ILLO	Upper Grits Pisolithic and Nodular Clays Lower Grits		
PRECAMBRIAN	BASEMENT COMPLEX			

Tertiary Rocks

Tertiary deposits are classified into the following categories, ranging in age from more experienced to more youthful: (1) the majority of the Middle Eocene rocks are formed of sandy shale that is connected to the Paleocene of Kalambaina formations and shallow marine limestone with White clayey limestones and shales with rich fossils. (2) Paleocene rocks, in accordance with Kogbe (1979), the Ostracords, and Bivalves of the Kalambaina Formation, are divided into two parts: a lower marine grouping (marine deposits) and an upper fluvial non-marine deposits (late Paleocene, Landenian age). The Paleocene strata in the area under study are made up of undifferentiated White Clayey limestones and grey laminated shales containing a lot of fossils.

Quaternary rocks

According to Kogbe (1981), the Quaternary deposits can be divided into two groups: Eocene deposits and Miocene ones. The Continental Terminal, red molted massive clays with sandstone intercalation, and ironstone are among the deposits from the Eocene period found in the Gwandu region. On the other hand, deposits from the Miocene period have an arrangement of loose sediments that have accumulated due to unstable environmental conditions. Sand dunes, coastal sand, and silts are among them (Kogbe, 1981).

MATERIALS AND METHODS

Digital filtering tools used for data processing in the study area

Many techniques can be used to distinguish the regional from the residual component. Here, the inversion process typically entails a computer-based Fourier Transform method that includes enhanced First vertical derivative, Spectral depth analysis, Upward continuation, Standard Euler deconvolution techniques and 3D Interface-Based Inversion (Spector and Grant, 1970), as well as the improvement methods. These inversion methods utilize the potential field data and transform them into a 2D or 3D subsurface spatial distribution of densities and susceptibilities or a subsurface topographical undulation, which then results in the observed gravity and magnetic anomalies. All of the methods are briefly discussed below.

Science World Journal Vol. 18(No 4) 2023 DOI: https://dx.doi.org/10.4314/swj.v18i4.2
www.scienceworldjournal.org
ISSN: 1597-6343 (Online), ISSN: 2756-391X (Print)
Published by Faculty of Science, Kaduna State University

First Vertical Derivative (FVD)

This improvement method is used to the Bouguer/TMI anomaly map in order to sharpen abnormalities and enable sharper vertical imaging of the causal structures. When the first vertical derivative filtering technique was used, it strengthened the high frequency components at the expense of the deep-seated low frequency components. The gravity or magnetic field's amplitude spectrum was multiplied by a factor of the following form to obtain the first vertical derivative of the gravity/magnetic field data (Salem et al. 2002).

$$FVD=\left(\frac{\partial F}{\partial Z}\right) \quad (1)$$

It works well for separating lineaments and contacts that are close to the surface.

Total horizontal derivative of tilt angle

To map shallow basement formations and mineral exploration targets, total horizontal derivatives of tilt angle are utilized (Hinze et al., 2013); the derivatives are also employed for enhancing characteristics and causing anomalous behavior, and body edge detection in potential field images. The tilt of angle filter was proposed by Miller and Singh, (1994) and further developed by others, including Salem et al., (2002); (2007). Because of its inherent simplicity and usefulness, it attracted a lot of attention (Hinze et al., 2013). In contrast to the local phase, the tilt of angle derivative (TDR) uses the absolute value of the total horizontal derivatives (THDR), all amplitudes are constrained to values between + $\frac{\pi}{2}$ and - $\frac{\pi}{2}$ (+90° and -90°), because of the nature of arctan trigonometric function (Salem et al., 2007).

The zero crossing of tilt derivative is found close to the borders of the model structures. The tilt derivative differs noticeably with inclinations of 0° and 90°. Positive values are situated above the sources, whilst negative values are situated below them. Moreover, the depth to the top of the contact or the half distance between the -45° and 45° is also equivalent to the horizontal distance from 45° to 0° (Hinze et al., 2013; Salem et al., 2007). Similar to the analytic signal, the total horizontal derivative of the tilt angle (THDR_TDR) is inclination- independent and sharper, producing more defined Maxima situated over the body edges. These maxima endure to thinner features until aggregating into a single peak.

Spectrum analysis of potential field data

The spectrum analysis of potential field data is built on the Fast Fourier Transform (FFT). Radially averaging is used to construct the energy spectrum using the Geosoft Oasis Montaj mag-map technique. According to Likkason (2015), the FFT converts grid data from the space domain to the Fourier wavenumber domain. Filters are used in the Fourier wavenumber domain in mag-map. The space domain function f (x, y)'s Fourier transform is mathematically described as follows:

$$F(\mu, v) = \int_{-\infty}^{\infty}\int_{-\infty}^{\infty} f(x,y).\, e^{i(\mu x+vy)}dxdy \quad (2)$$

Its inverse is expressed as:

$$f(x,y) = \frac{1}{4\pi^2}\int_{-\infty}^{\infty}\int_{-\infty}^{\infty} F(\mu, v).\, e^{-i(ux+vy)}dudv \quad (3)$$

Where u and v are wave numbers (in radians per ground units) in the x and y directions respectively (here x and y are in ground units) and i = √-1. These are related to spatial 'frequencies' f_x and f_y in cycles per ground unit (Naidu, 1969).

A given potential field function in the wavenumber domain has a single, separate function, and vice versa. The plotting of energy against wavenumber and direction forms the two-dimensional function known as the energy spectrum. A spectrum can be used to explain how energy changes depending on wavenumber. The expression in equation (3) describes the relationship between the power spectrum $|f(\mu, v)|^2$ and its total energy E_T:

$$E_T=\frac{1}{2\pi}\int_{-\infty}^{\infty}|f(\mu,v)|2\ d\mu dv \quad (4)$$

where x- and y-directional wavenumbers are μ and v, respectively. In contrast to the limitless region assumed in mathematical equations (2), (3), and (4), geophysical potential field gravity data are collected with fixed limitations within the study area. Since depth requires imaging deeper features, the study area should be significant and be produced by radially averaging the energy spectrum. The only factor affecting the radially averaged energy spectrum is wavenumber. The spatial frequency of a wave, expressed in cycles per unit distance, is known as wavenumber k. The greatest frequency that can be measured with a fixed sample interval is the Nyquist wavenumber N, which is the largest wavenumber that has been sampled by the grid. Thus:

$$N=\frac{1}{2d} \quad (5)$$

Where d is the sample interval, the expression in equation 8 determines the depth of a statistical ensemble of sources (Naidu, 1969) as:

$$LogE(r)=-4\pi hr \quad (6)$$

Where h is the depth in ground units and r is the magnitude of the wave number in cycles/ground unit. Thus one can determine the depth of an "ensemble" of sources by measuring the slope of the energy (power) spectrum and dividing by 4π and so various straight segments of the line spectrum represents various ensembles of sources (Spector & Grant, 1970).

Standard Euler deconvolution techniques

Thompson (1982) describes a method which applies Euler's equation to successive segments of a pole-reduced profile of magnetic data, solves for source position, and obtains an indication of source type. Any 3D function f(x, y, z) is said to be homogeneous of degree n if the function obeys the expression:

$$f(tx,ty,tz) = t^n f(x, y, z) \quad (7)$$

From equation (3.29), it can be shown that the following (known as Euler's equation) is also satisfied:

$$x\frac{\partial f}{\partial x} + y\frac{\partial f}{\partial y} + z\frac{\partial f}{\partial z} = nf \quad (8)$$

Considering potential field data, Thompson (1982) showed that Euler equation of (8) known as the 3D Euler's homogeneity relation could be written in the form:

$$(x - x_0)\frac{\partial T}{\partial x} + (y - y_0)\frac{\partial T}{\partial y} + (z - z_0)\frac{\partial T}{\partial z} = N(B - T) \quad (9)$$

Where (x_0, y_0, z_0) is the position of a magnetic source whose total field, T is detected at (x, y, z). The total field has a regional value B. The degree of homogeneity, N (equivalent to n in the Euler's equation) may be interpreted as a structural index (SI), which is a measure of

Science World Journal Vol. 18(No 4) 2023 DOI: https://dx.doi.org/10.4314/swj.v18i4.2
www.scienceworldjournal.org
ISSN: 1597-6343 (Online), ISSN: 2756-391X (Print)
Published by Faculty of Science, Kaduna State University

the rate of change with distance of the field. For example, the magnetic field of a point dipole falls off as the inverse cube, giving a structural index of 3, while an effective vertical line source such as a narrow, vertical pipe gives rise to an inverse square field, giving an index of 2. Extended bodies are assemblages of dipoles and have indices ranging from zero (infinite sheet) to 3. Thompson (1982) suggests that the index for a magnetic contact is less than 0.5. This value often leads to underestimation of depth, even when testing ideal models (Reid et al. 1990). For structural index of zero, Reid et al. (1990) have shown that the appropriate Euler's equation is then:

$$(x - x_0)\frac{\partial T}{\partial x} + (y - y_0)\frac{\partial T}{\partial y} + (z - z_0)\frac{\partial T}{\partial z} = A \quad (10)$$

Where A incorporates amplitude, strike and dip factors which cannot be separated easily.

Given a set of observed total field data (or the anomaly data), we can determined an optimum source location (x_0, y_0, z_0) by solving the 3D Euler's equations for a given index N by least squares inversion of the data. The inversion process will also yield an uncertainty (standard deviation) for each of the fitted parameters, and this can be used as a criterion to accept or reject a solution. This inversion process is often called Euler Deconvolution.

Equations (9) and (10) are easily applied to gridded data. The steps in the process are as follows:

(a) Calculate (or measure) the gradients: $\partial T/\partial x, \partial T/\partial y, \partial T/\partial z$

(b) Locate a square window within the grids of gradient values and field values of the size of at least 3x3 grid points. The window is centred on each of the solution locations. All points in the window are used to solve Euler's equation for solution depth inversely weighted by distance from the centred of the window. Hence the window should be large enough to include each solution anomaly of interest in the total field magnetic grid, but not large enough to include any adjacent anomalies. Usually 10 x10 window is chosen for good result and provides 100 equations from which four unknowns (x_0, y_0, z_0 and B) and their uncertainties (standard deviations) are obtained.

(c) For SI of zero, proceed as for (b) above, but using equation (10) and solve for source position and the arbitrary offset value A

(d) Repeat steps (b) and (c) for some or all the possible window positions, including overlaps

(e) Plot maps of the solutions for each structural index (SI) plotted at its plan (x, y) position using a symbol size proportional to depth z.

(f) After examining results, one may want to eliminate spurious solutions by windowing on either depth (or elevation), x and y offset or on the uncertainties (in depth or location) by trial-and-error schemes.

(g) In interpreting results from Euler deconvolution analysis, the posers are: (1) are the geologic features of interest represented in the results? and (2) for a given feature, is the structural index correct?

Euler Deconvolution is a statistical process and so the resulting solutions have associated uncertainties which must be acknowledged and discussed.

RESULTS AND DISCUSSION

Two distinct types of geophysical maps were used. The first type depicts the Bouguer gravity anomaly map in the Southeastern portion of Iullemmeden Basin (NW, Nigeria) (Figs. 3a), while the others depict the magnetic anomaly map of the study area (Fig. 3b), which was created using the same methodology described by Adamu et al. (2022), but updated the gravity dataset in interest of the region with free access download websites of the United State Geological Survey, USGS, and International Gravity Bureau IGM, which maintain the World Gravity Model, (WGM 2012). The Earth Gravity model, EGM 2008, satellite gravity and the Topography 1 arc-minute (ETOP1) database for topography were used to calculate and produce (Fig. 3a). This will serve as the harmonic coefficients for an expansion of spherical harmonics up to an order of 10, 800 in order to create the Earth's Topography derived gravity model at 1' x 1' resolution (ETOPG1) model. On the other hand, the research area's reduced to equator magnetic anomaly map (Fig. 3b) is identical to that of Adamu et al. (2022); in this instance, the beginning point is the northern portion of the Kebbi, Sokoto, and Zamfara magnetic map (KSZMMP) (NGSA, 2010), resulting in a simple arithmetic addition of 33,000 nT to each value of Z column, the specifics of the processing methods in both circumstances are detailed in Adamu et al. (2022). The gravity anomaly map for the current study and its surroundings is the consequence of adjoining regions in the Northern and Southern regions that point toward the Niger Republic (Fig. 3a). The research area's magnetic anomaly, RTE map (Fig. 3b) was created using high-resolution aeromagnetic information over the sedimentary basins. The high-resolution datasets are the outcome of various aeromagnetic surveys conducted by the Nigerian Geological Survey Agency, NGSA. Line spacing and flying height are usually 500 and 100 meters, respectively. Note that Figure 3b, is a reduced-to-the-magnetic-equator map, clearly showing a low latitude region, which will help us better correlate gravity and magnetic anomalies.

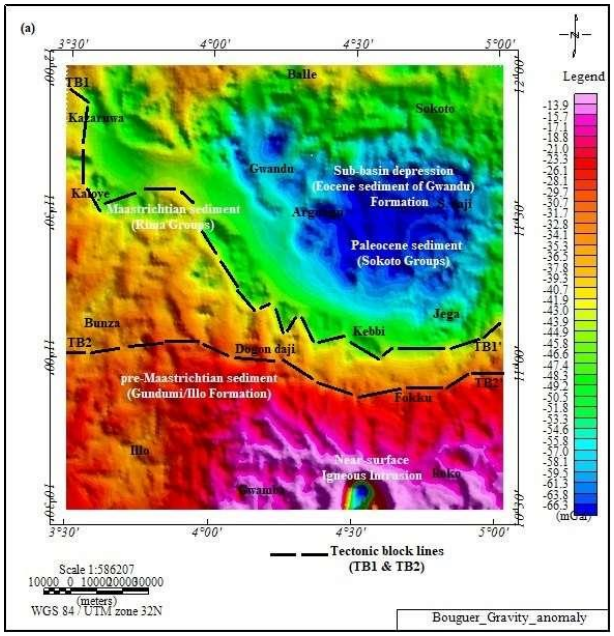

(a)

Science World Journal Vol. 18(No 4) 2023 DOI: https://dx.doi.org/10.4314/swj.v18i4.2
www.scienceworldjournal.org
ISSN: 1597-6343 (Online), ISSN: 2756-391X (Print)
Published by Faculty of Science, Kaduna State University

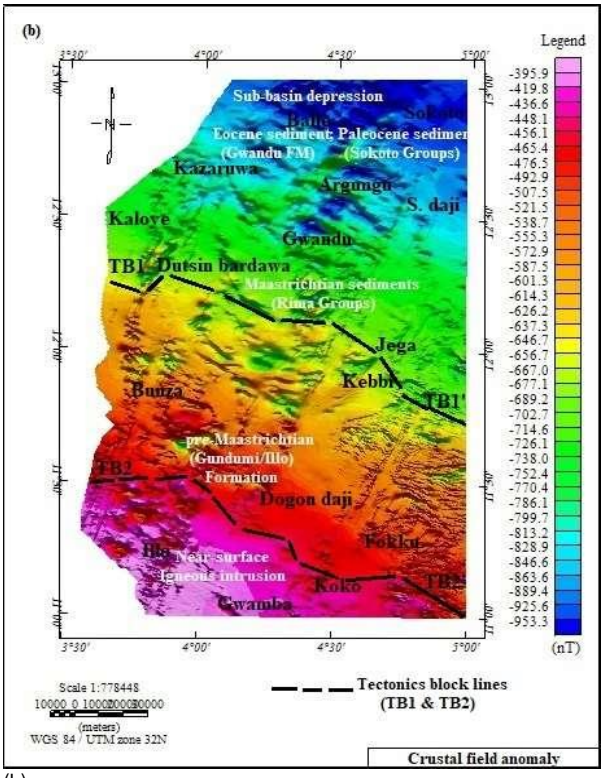

(b)

Figure 3: (a) Bouguer gravity anomaly image of the study region acquired from the World Gravity Model (WGM, 2012) overlaid with Geosoft Oasis montaj version.8.4 (b) Crustal field anomaly map of the study region scaled to magnetic equator, (RTE) projected onto Geosoft Oasis montaj version.8.4.

Improved use of aeromagnetic and Satellite gravity data based on enhance gradients

Within the study areas of sediment infill zones, the reduced to equator RTE magnetic anomaly map revealed a magnetic minimum of -953.3 nT (Fig. 3 a,b). The results, on the other hand, revealed magnetic maxima of -395.9 nT to the north and minima to the south, particularly within the northern half of the Sokoto Group and the northwestern boundary of the Duku-Tarasa (escarpment features). The Bouguer anomaly map was utilized to depict the formation's boundaries throughout the Sokoto basin, with gravity minima of (-66.30 mGal) and peaks of (-13.90 mGal) (Fig. 3 a,b). Vertical derivatives were generated from Bouguer and aeromagnetic anomaly maps in order to refine the borders of causative anomalous bodies (Figs 4a and 4b). Vertical derivatives, for example, are useful for establishing the breadth and enhancing the source edge bodies. Furthermore, vertical derivatives may be more effective at enhancing shallower density sources than horizontal derivatives. This is seen in (Fig. 4 a, b), which exhibits shallower sediment infill inside the Sokoto Group zone that is better resolved than the blocks of the study region that slope northwest to southeast. Vertical derivatives are likewise demonstrated to be positive around the borders of the sub-basin depression zone and within the escarpment features. Vertical derivatives identify shallower sediment filling, which predominates in the study area's northwest and a few tiny locations within the basement intrusion zone. A horizontal gradient maxima 1.37 nT/m across the borders of the basement outcrop, both of which are near to the E -to W- trending normal fault of Anka-Yauri-Zuru, which is found between the southwest part zones, and the gradient is zero over the zone itself (Figs 4 a,b). However, if there are many causes for this anomaly, the shallower sources will be easily resolved, whereas the deeper sources with shallower gradients may not be as visible because gradient amplitude is the important indicator (Adamu et al., 2020; Likkason, 2014; Nabighian, 1972, 1984).

The primary magnetic gradients were disclosed by the total horizontal derivative of tilt angle (THDR_TDR), as well as the presence of these gradients on the map identifying clear boundary of Gwandu and Gundumi/Illo formations which composed of ferruginous materials (Fig. 4c). In the SE part of THDR_TDR map, the boundaries of the magnetic intrusive bodies (intra-sedimentary) of Gundumi/Illo Formations and ferruginous materials of Gwandu and Taloka Formation were depicted. No discernable feature/boundary was shown for both Rima and Sokoto groups because the spectrum could not pick up clay and sand (Fig. 4c).

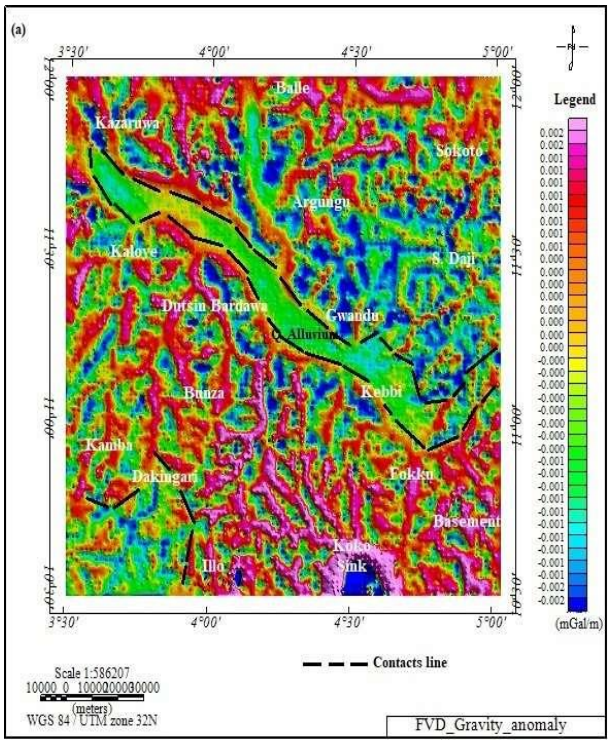

(a)

Science World Journal Vol. 18(No 4) 2023 DOI: https://dx.doi.org/10.4314/swj.v18i4.2
www.scienceworldjournal.org
ISSN: 1597-6343 (Online), ISSN: 2756-391X (Print)
Published by Faculty of Science, Kaduna State University

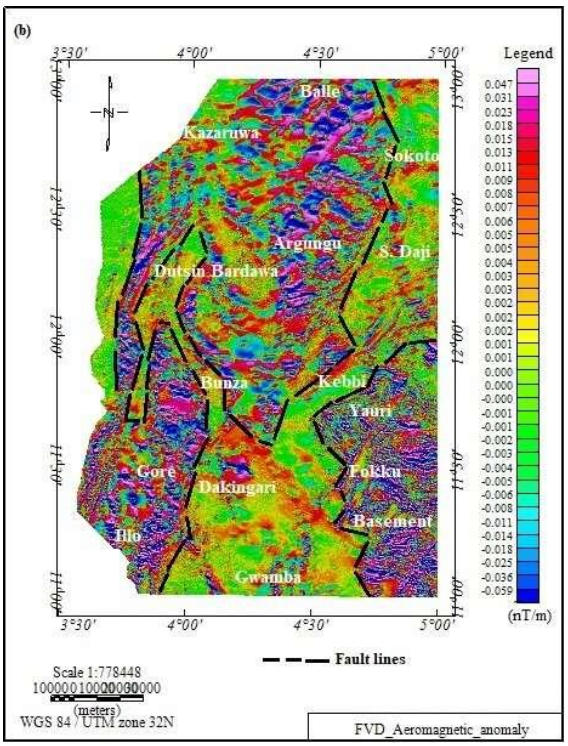

(b)

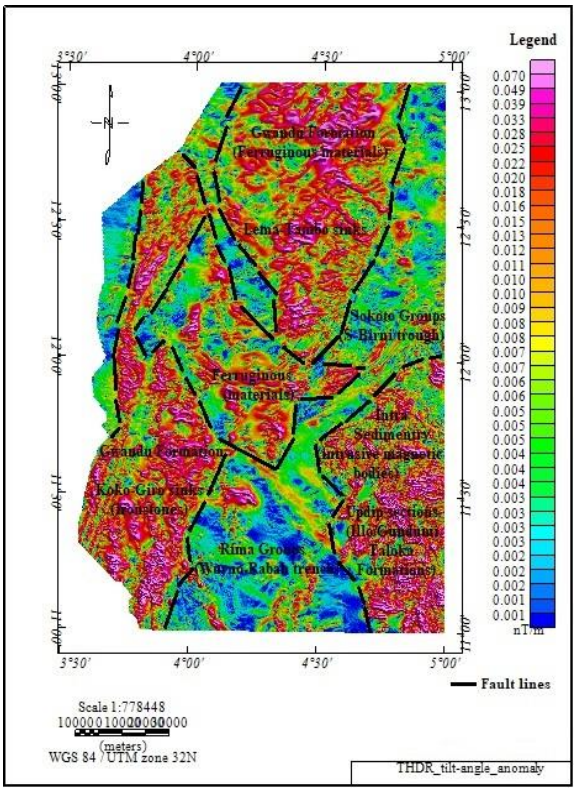

Figure 4: Derivatives maps of the study area deduced from first vertical gradient (a) aeromagnetic data (b) gravity data (c) Tilt-angle anomaly

Upward trend of satellite gravity data

The Tertiary sediment infill of the Sokoto and Rima Groups as well as Gundumi and Illo Formations are exposed where the Bouguer gravity anomaly map (Fig. 3a) shows a gravity minimum (-66.31 mGal). The Gulma region, Arewa-Jantulu, and Duku-Tarasa escarpment features are all shown to have a gravity maximum (-13.94 mGal) on the Bouguer gravity anomaly map. In order to determine the potential depth at which the Cretaceous to Tertiary layers may have an impact on the Bouguer gravity anomaly, an upward continuation was applied to (Fig 3a). the upward continuation requires that the gravity field be mathematically extended from a particular shallower depth to a particular deeper depth in order to remove the influence of near-surface and shorter wavelength anomalies (Demissie et al., 2018; Jacobsen, 1987; Zeng et al., 2007; Adamu et al., 2022). Demissie et al., (2018), made used of the upward extension of the gravitational field anomaly up to a specific height (Z) where the source depths are equal to or less than half of the extension depth. The Bouguer gravity anomaly data were consequently increased to heights of 7 km (Fig. 5a), 20 km (Fig. 5b), 30 km (Fig. 5c) and 40 km (Fig. 5d). The anomalies on these several maps have a source that can be roughly found at or below depths of 3.5 km, 10 km, 15 km and 20 km, respectively, while specific depth may not be accurate. The Upper crust of Cretaceous to Tertiary layers or other less dense sedimentary strata to depths of ~3.5 km and ~10 km, respectively, were indicated by gravity minimum on the 20 km and 30 km continuation height maps (Figs 5b and c). The 40 km upward continuation, however, revealed a broad gravity high of the Moho depth moving out rather than gravity minimum associated with a sub-basin depression (Fig. 5d). It is unlikely that the sediment filling of Cretaceous to Tertiary strata in the examined area is as thick as ~3.5 km given the geological constraints. Therefore, the interpretation of these results was merely indicating that the sediment filling of the study area is less than ~3.5 km thick.

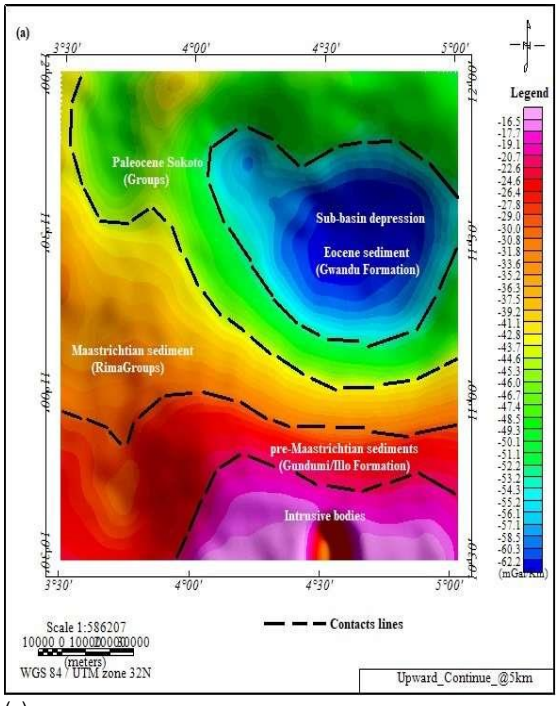

(a)

Science World Journal Vol. 18(No 4) 2023 DOI: https://dx.doi.org/10.4314/swj.v18i4.2
www.scienceworldjournal.org
ISSN: 1597-6343 (Online), ISSN: 2756-391X (Print)
Published by Faculty of Science, Kaduna State University

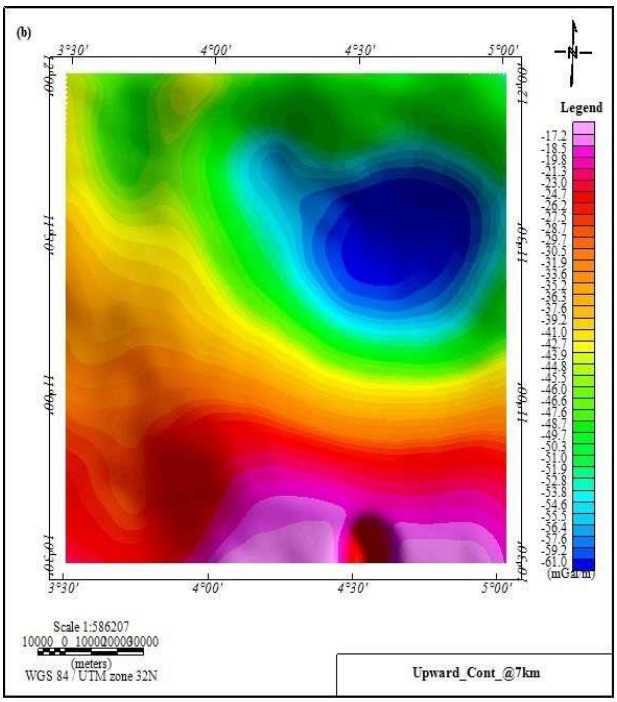

(b)

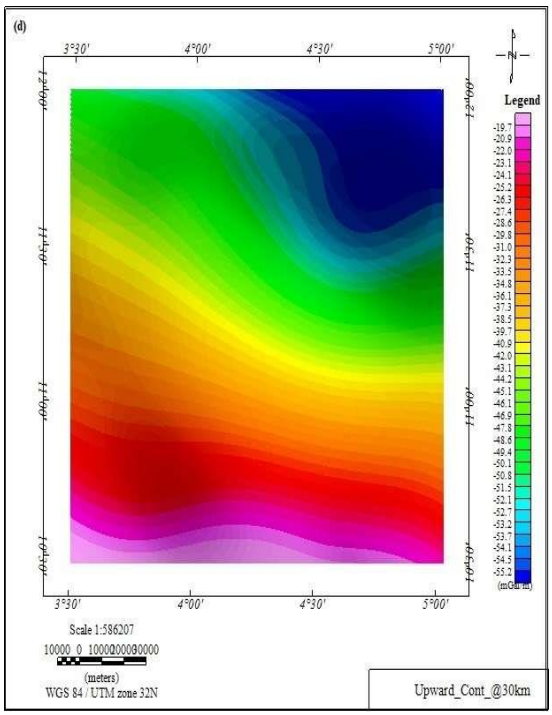

(d)

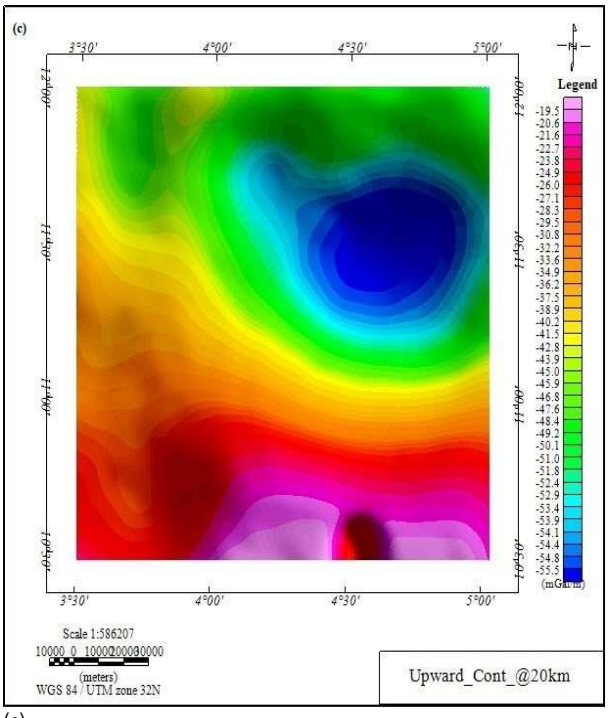

(c)

Figure 5: Upward continuation maps of regional trends over the study area's Bouguer anomaly generated from World Gravity Model (WGM, 2012), the Bouguer gravity anomaly was extended to a height of (a) 5 km (b) 7 km (c) 20 km; and (d) 30 km

Interpretation Approach

In order to examine the regional crustal structures of areas with distinct geological evolution its extensively studied using potential field data (e.g. gravity and magnetic). The evidence that the crustal structures may be linked to noticeably differing densities and/or magnetizations between distinct crustal domains, as well as by geophysical signals along the structures dividing these domains, forms the basis of the integrated geophysical interpretation (Adamu et al. 2022). The interpretation of magnetic anomalies followed the simple hypothesis that only induced magnetization was present. In crustal research, gravity regional records are frequently employed for a variety of reasons, two of which are largely technical. First, according to Blakely (1995), densities fluctuations are the primary cause of Bouguer gravity anomalies and the deeper the source, the longer the wavelength of the anomaly. Although it's not always the case, deep sources and/or shallow, big bodies can both contribute to huge wavelength anomalies. Similarly, gravity anomalies caused by crustal sources are therefore very thoroughly sampled, and to characterize forms of crustal heterogeneities, a minimum area of 10, 000 km^2 is required. The derivatives of the radially averaged power spectrum of the anomalies provide depth estimates to the sources under the model where regional sources are produced by the union of laterally juxtaposed vertical prisms (Spector and Grant, 1970; Blakely, 1995; Likkason et al. 2013). It should be noted that the contributing sources include even the heterogeneities of the lithostratigraphic formations due to their top depth of up to 30 km (Fig. 5d). The resolution to define lateral fluctuations of density is quite good, which is the second factor that contributes to the gravity regional datasets

Science World Journal Vol. 18(No 4) 2023
www.scienceworldjournal.org
ISSN: 1597-6343 (Online), ISSN: 2756-391X (Print)
Published by Faculty of Science, Kaduna State University
DOI: https://dx.doi.org/10.4314/swj.v18i4.2

extensive application in crustal studies (Demissie et al. 2018). Due to these two technical factors, regional maps of Bouguer gravity anomalies can be used to identify deep-rooted crustal compartments of different densities quite accurately. The same technical justifications outlined above for widespread use of gravity datasets also apply to magnetic datasets, with the exception of the restrictions that the maximum depth contributing sources of magnetization is the crustal mantle depth (Moho) or Curie point depth and the challenges associated with magnetic anisotropy and remanence (Blakely, 1995).

Quantitative Interpretation

The quantitative interpretation to estimate or picture the underlying structure uses the Euler deconvolution, power spectrum analyses, and 2D forward modeling. The power spectrum analysis is utilized to determine the depth of the subsurface source and any potential interfaces, while the Euler deconvolution is employed to resolve the 3D components of structural features

Spectrum analysis of potential field gravity data

It is common practice to calculate first-order depth estimates to magnetic susceptibility and density interfaces using spectrum analysis of magnetic and gravity data (e.g., Demissie et al. 2018; Likkason et al. 2015). The satellite gravity and aeromagnetic data were utilized to perform a spectral analysis, applying the spectral analysis approach described by Likkason, (2013) and Tanaka et al. (1999), to estimate the depth to subsurface boundaries beneath the research region and its environs. This analysis was established at five (5) randomly scattered around the research zone, as shown in figure 2b. Each location point has a 10 km horizontal line midpoint, and each profile was designed to include lines of (L_1-L_1', L_2-L_2', L_4-L_4', L_6-L_6' and L_7-L_7'), the centers of which were used to indicate the Moho (deep), lower to upper crust (intermediate), and sediment thickness (shallow). Figures (6a, b, c) depict a series of spectral analysis curves from 1 to 10 using the natural logarithm of the power spectrum versus the wavenumber, indicating how the value of the power spectrum varies as more and more points are observed in line with one another. For each profile (L_1, L_2, and L_4, L_6 and L_7), the depth due to gravity sources was calculated using the radial power spectrum-based slope of the curves.

The Moho (deeper source), as demonstrated by the structure of low wavenumber power spectra curves, was assumed to exist. Figures 6 (a-c) indicate the shallow to deep gravity sources of the research area on maps. The highest depth of a shallow gravity source, Continental Terminal, is 4.79 kilometers below the surface (Adamu et al. 2022). In general, this depth increases from East to West. A similar growing trend pattern can be seen on the map of the deep gravity source (Moho depth), which has a maximum depth of 14.34 km below the surface (intermediate, Lower to upper crust). Figure 6d depicts a generalized 3D representation of how the shallow and deep gravity sources spanning the Gwandu Formation, Gundumi and Illo Formations, and the Sokoto Group interact with the surface topography throughout the basins. In compared to the deep source, which has a radius of 10 km, the basin area has a wider radius and is flatter, showing a typical downhill fundamental structure. The drapes of solid black line indicate the main Quaternary alluvium's downward expansion across the formation, which is linked to the normal fault line (Kogbe, 1979). Figure (6e) depicts five profiles L_1-L_1', L_2-L_2', L_4-L_4', L_6-L_6', and L_7-L_7'), over the terrain, as well as shallow and deep source maps (Figures 7a, b, c).

According to these profiles (Table 3), the deepest section, with an

The highest mean depths of the top magnetic sources are fact around 45.75 km, as shown by the generated two-dimensional (2D) deeper map of radially averaged power spectrum (Fig. 6a; Fig. 6b), which can be used to determine the Moho, Lower and Upper crust depth for the research area. Magnetic information can therefore be used to identify crustal boundary with different magnetism. In order to identify the structures connected to geophysical contrasts into the two categories of major and minor ones, the shear zones and main contacts on the vertical derivative maps were first superimpose.

average depth of 22.86 km, is nearly in the middle of the profile, where the majority of the formations, lithological connections, and weak zones were discovered. Without including ferruginous elements, the graphs' trend (fig. 6e) similarly illustrates the sediments' propensity to thin out toward the northern portion of the research region (coastal) in the areas of Argungu, Gulma, Sabiyel, Aliero, Jega, Bunza, Birnin Kebbi, and Makera. This demonstrates that subsurface features have a substantial impact on groundwater or hydrocarbon accumulation investigations in the examined location.

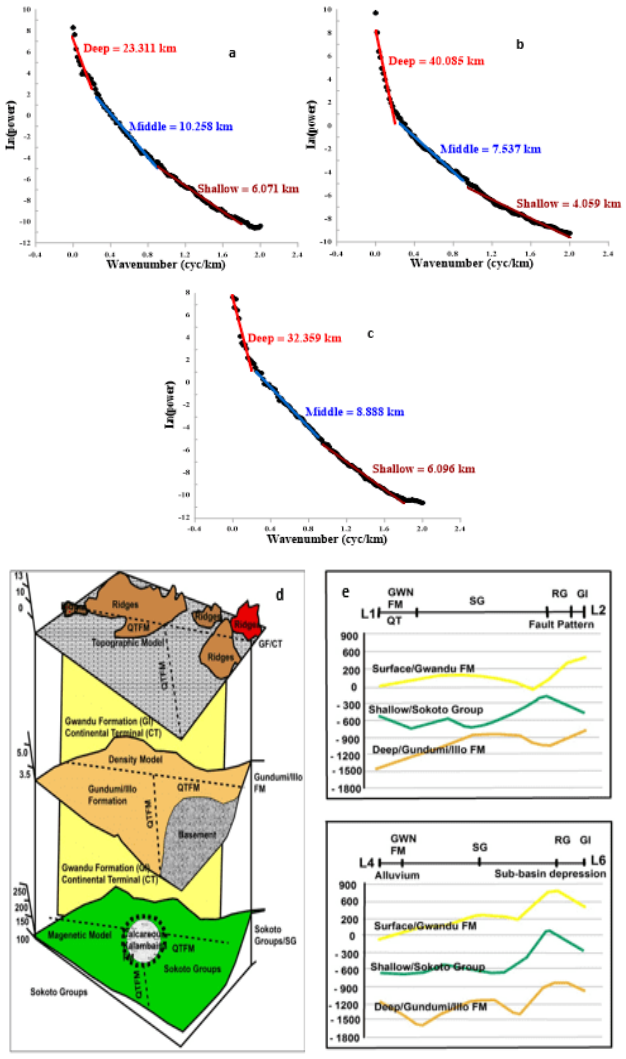

Figure 6: (a, b, c) an examples of log spectral powers versus wavenumber of blocks L_1, L_2, L_4, L_6 and L_7, profiles (d) 3D overview

Science World Journal Vol. 18(No 4) 2023 DOI: https://dx.doi.org/10.4314/swj.v18i4.2
www.scienceworldjournal.org
ISSN: 1597-6343 (Online), ISSN: 2756-391X (Print)
Published by Faculty of Science, Kaduna State University

of the deep and shallow magnetic-gravity sources, trends with topography, indicates the extension of the various formations, basement and the quaternary line downward the sub-basin depression (e) Established profiles of L_1, L_2 and L_4, L_6 across the topography with shallow and deep source maps.

The Standard Euler deconvolution

To locate faults/lineaments contacts with depth estimates based on Euler anomalies, Euler's solutions of the bouguer anomaly map are created in this work using structural indices of --0.5, 0, -1, 1, and 0.5. Grid cells with 10 km by 10 km and 20 km by 20 km window sizes and a 7% depth of tolerance were utilized (Table 2). The fault/lineaments known to exist in the Sokoto Basin were adopted from the geological map, and when both maps were layered on top of the extracted lineament map and the northern portion of the Quaternary alluvium, a considerable number of Euler anomalies were discovered. There is a scattered concentration of Euler anomalies near the western and eastern margins of Sokoto and the Rima Groups.

The Sokoto Group, which includes the Gamba Formation, has the highest number of Euler anomalies along the fault zone. These formations are shallow in the north, ranging from 98.73 to 6548.80 m (contact) of profile L_4, and deeper in the south, ranging from 402.50 to around 4550.34 m (dykes) of L_4. An intrusion of basement outcrops separates the Gundumi and Illo formations from another significant fault boundary at a shallow depth of 209.01 to more than 3284.92 meters (contact), and it gets deeper as it moves toward the southeast with a depth range of 5237.00 to about 20925.11 m, which separates the Illo Formation and the basement intrusion. However, the solutions are heading in the following directions: NW-SE, ENE-WSW, E-W, and NE-SW. Furthermore, Euler anomalies have been observed in the western half of the Sokoto groups, which may represent a contact boundary between Quaternary sediments and the Gwandu Formation. Table 2 summarizes the depths of information for the Euler solution of profiles L_1, L_2, L_4, L_6 and L_7 in the study area.

Table 2: Depths to gravity anomaly sources of Euler deconvolution for profile L_1, L_2, L_4, L_6 and L_7, with structural index of 0, 1, 7, 10 (contact) and -0.5, -1, 7, 10 (dykes) in the area of study.

S/N	Profiles	Parameter	Depth (minimum) (m)	Depth (maximum) (m)		Depth (mean) (m)	Standard deviation (m)	Remark
1	L1	Z_Contacts	-911.51	-8575.17		-1692.2	788.62	Estimates depth and position of causative body
		Z_Dykes	-4025.39	-5645.99		-1230.33	665.96	
2	L2	Z_Contacts	-1329.20	-3687.28		-842.86	397.09	//
		Z_Dykes	-123.10	-4838.10		-516.40	378.61	
3	L4	Z_Contacts	-98.73	-6548.80		-1238.37	637.44	//
		Z_Dykes	-4020.50	-4550.34		-902.09	478.66	
4	L6	Z_Contacts	-133.37	-6261.85		-1303.07	585.79	//
		Z_Dykes	-4902.97	-0.15		-193.01	99.94	
5	L7	Z_Contacts	-209.01	-3284.92		-174.69	366.21	//
		Z_Dykes	-5237.00	-20925.11		-130.81	422.31	

Depth to the density and magnetic sources

Using the reduced to magnetic equator anomaly of aeromagnetic data covering the Southern part of Kebbi, Sokoto, and its environs, we computed the 2D spectrum for 0.4° × 0.4° (∼ 80 km ×∼ 80 km) window. The window has been widened by 30% to compute the magnetic susceptibility sources close to the edges and avoid the edge effect (Gibb's phenomena) while applying the Fast Fourier Transform, the window (Likkason et al. 2013; Tanaka et al. 1999). The depths to the top of the magnetic interfaces are determined based on breaks in the slope of the logarithmic plot of the 2D spectral curve (Fig. 6a). Then, a linear segment with a slope associated to magnetic interfaces can be used to estimate the region between the slope breaks. The user-detected breaks in the slope of the 2D spectral curve are what determine which linear segments should be used. Using several radial angular frequency ranges to estimate a variety of slopes (Table 3). Using Excel's linear function, which is based on the least squares best fit technique, the difference between these linear segments and the actual data were then calculated. The depth to the magnetic contact was determined using the average slope from these slope calculations (Table 3). To estimate the potential error in our depth estimates, the technique described by Dimissie et al. (2018), were used. In this method, the error is defined as the ratio of the standard deviation of the linear fit to the range of the wavenumbers used to calculate the slopes for each interface from the 2D spectral curves. The 2D spectral curve in figures 6a,b,c, suggest that magnetic boundaries exist at depths of ∼40.09 km, ∼32.36 km, and ∼23.31 km, which correspond to low (0.03 – 0.25 radian/km), intermediate (0.25 – 0.35 radian/km) and high (0.35 – 0.45 radian/km) radian angular frequency respectively. The predicted Moho depth from the analysis and the 23.31 km depth are in good agreement with (Likkason et al. 2014). However, because to numerous studies concluding that magnetic data is of limited help in imaging abnormalities below the Lower crust/Curie point depth, inferring that the Moho were shown by this depth is something hesitant to do (Likkason et al. 2013; Salem et al. 2014). According to our interpretation, the lower and upper crustal boundaries lie at a depth of ∼8.9 km. In earlier research, the depth corresponding to high wavenumbers was thought to correlate to near-surface random noise. However, the 4.09 km depth is consistent with the depth to the Pre-Maastrichtian sediments of Gundumi and Illo formations, which has been calculated geological observations by (Kogbe, 1981). The spectral analysis technique, first developed by Spector and Grant (1970), has since been widely adopted by many researchers (e.g., Likkason et al. 2013; Likkason, 2011) to determine the depths to density interfaces beneath the Southern

Science World Journal Vol. 18(No 4) 2023 DOI: https://dx.doi.org/10.4314/swj.v18i4.2
www.scienceworldjournal.org
ISSN: 1597-6343 (Online), ISSN: 2756-391X (Print)
Published by Faculty of Science, Kaduna State University

part of Kebbi, Sokoto and its surroundings. In order to reduce Gibb's phenomenon, we calculated the 2D spectrum for a 1° × 1° (∼100 km ×∼100 km) window with the Southern half of Argungu as the centre and 50% grid expansion in all directions. The satellite gravity data were subjected to the same statistical analysis as previously discussed. According to the 2D spectral map, density boundaries at depths of ∼14.20 km, ∼6.48 km, and 4.79 km corresponding to low (∼0.03–0.04 radian/km), intermediate (0.10–0.32 radian/km) and high (∼0.33–0.40 radian/km) wavenumbers. In good agreement with the depth of ∼18.57 km found by Nwanko and Shehu, (2015), from the southern section of the Sokoto Basin, the depth ∼23.31 km was interpreted as depth of the Moho (Table 3).

Table 3: Depths and density information from spectral blocks analysis for gravity and magnetic used for the development of 2D deeper map (Moho), Lower and Upper crust.

S/N	Spectral Blocks	Depth to (Moho) (m)	Depth to (L & U crust) (m)	Density (g/cm^3)	Magnetic (Susceptibility) (SI)
1	B1	45.75	14.34	5.30	1.501E-05
2	B2	22.98	13.80	2.00	1.201E-05
3	B3	23.36	12.58	3.62	1.303E-03
4	B4	23.31	10.29	2.96	1.050E-03
5	B5	25.44	9.62	2.67	1.123E-03
6	B6	26.99	9.26	1.86	1.022E-03
7	B7	32.36	8.89	2.43	2.721E-02
8	B8	26.48	9.03	2.46	2.120E-03
9	B9	28.06	6.48	3.12	1.214E-05
10	B10	16.46	6.94	1.74	1.106E-03
11	B11	40.09	7.54	1.99	1.321E-01
12	B12	27.34	4.79	1.52	3.218E-03

Modeling in two-dimensions of gravity and magnetic covered for profile L_1 and L_2

The magnetic susceptibility and Bouguer gravity anomaly values that were computed and observed for the research area and its surrounds, as well as an idealized near-surface cross section, are depicted in the 2D model that was created for the area and its environs (Fig. 7). The model's length is about ∼ 40 km, and its major trends are aligned in an east-west direction that is roughly parallel to the strike direction of the Anka-Zuru-Yauri within the Sokoto basin (Fig. 1). Starting from the Eocene strata of the Gwandu Continental Terminal and extends southwestward into the Maastrichtian layers of Rima Group. The model is made up of four components; alluvium, Gwandu Formation, Rima Group, the lower and higher mantle crust, mafic dykes and the lithologies at the contact points between them possibly present. Table 3 list the magnetic susceptibility and density values for various model components. The aeromagnetic anomalies Root Mean Square Error (RMSE) between the observed and the estimated anomalies of the model is 2.032 nT (Fig. 7a_1, L_1) and the Bouguer gravity anomalies 0.3086 mGal (Fig. 7a_2, L_2). The Eocene strata of the Gwandu Formation's continental terminal contain the sediment filling. The sediments was divided into two layers, with thicknesses varying from ∼4.06 km at the border faults to ∼ 7.54 km close towards the Gwandu formation (Fig. 7a_4). With an average density of 2.43 g/cm^3, the sediments from the Gwandu Formation and the Maastrichtian layers of Rima Group were modeled (Table 3). The sediment filling of the Maastrichtian Taloka Formation, on the other hand, was given a lower magnetic susceptibility (1.501E-05 SI) than the Rima Group (2.120E-03 SI) (Table 3). The magnetic susceptibility value were ascribed to the Rima Group sediment filling in line with what is typical for lacustrine shales. Although it is higher than what is typical for lacustrine sediment, the magnetic susceptibility value attributed to the sediment filling of the Continental Terminal, Gwandu Formation. The sub-horizontal layer made up of 4 polygons, has an average thickness of ∼ 4.06 km and extends ∼ 7.5 km beneath the Continental Terminal, this is a results of the Formation's hanging wall downward plunge (Fig. 7a_3 and a_4). All of the polygons in the Gwandu Formation were ascribed average densities of ∼5.30 g/cm^3, ∼3.62 g/cm^3 and ∼2.96 g/cm^3, respectively; however these polygons also had magnetic susceptibility values that ranged from 1.201E-05 SI and 2.721E-02 SI (Table 3). This variation in magnetic susceptibility may be caused by differences in lithology, the existence of lateritic soil horizons in disproportion, and the degree of chemical weathering, which changes the spatial distribution of magnetic minerals (Adamu et al. 2021; Bonde et al. 2014). Additionally, the Rima Group varying in the magnetic susceptibility of the Rima Group can also be due to the commonly variable content of ferruginous materials within different Formations (Kogbe, 1979). The presence of various lithologies may have an impact on the variability of magnetic susceptibility values employed in our model, as demonstrated by the example that follows. For polygons in the Dukamaje and Wurno Formations of the Rima Group, the 2D model employs lower magnetic susceptibility values (Table 3, Fig. 7a_3 and a_4). The Moho depth was modeled as a homogeneous layer with depth varying from ∼40 km and ∼30 km (Fig. 7a4). Results from our spectral study of the aeromagnetic and satellite gravity data are in agreement with this (Fig. 7a, b, c). The lower and upper crustal mantle was given the density value of ∼2.67 g/cm^3 and a magnetic susceptibility value of 1.123E-03 SI. The carbonaceous mudstone,

Science World Journal Vol. 18(No 4) 2023 DOI: https://dx.doi.org/10.4314/swj.v18i4.2
www.scienceworldjournal.org
ISSN: 1597-6343 (Online), ISSN: 2756-391X (Print)
Published by Faculty of Science, Kaduna State University

ferruginous sand, and gysiferous shales of the Wurno, Dukamaje and Taloka Formations may make up the upper crust that lies beneath the Rima Group and its environs (Kogbe, 1981). The Rima Group Formations to the north and south, respectively, as well as the Gwandu Formation in the region of Sokoto Basin, has certain areas with these types of elements exposed. A model of the lower crust mantle was produced using three polygons to depict the lateral variation caused by zones of red molten massive clays with sandstone intercalation and ironstones (Fig. 7a$_4$). Our 2D model used depth range of ~ 23.31 to ~30 km for the Moho beneath the Maastrichtian strata of the Wurno Formation Rima Group and a depth of ~ 28 km for the Moho.

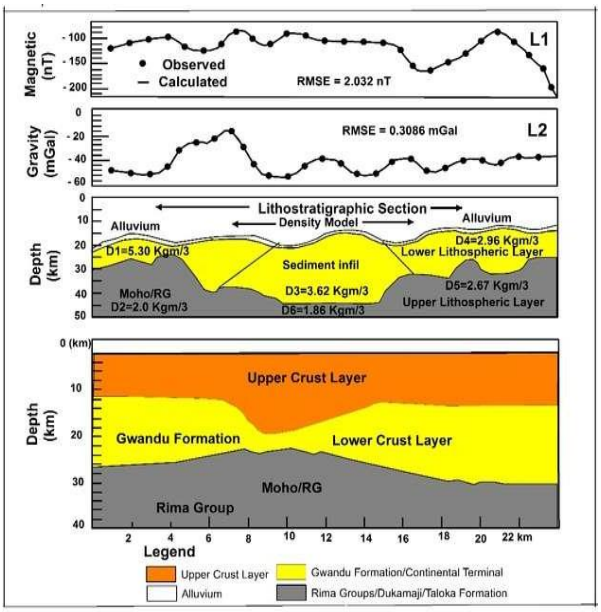

Figure 7: shows a two-dimensional (2D) forward magnetic and satellite gravity model of the crustal extension structures beneath the research area **(a$_1$)** magnetic anomalies were both measured from high-resolution aeromagnetic data and estimated for profile L$_1$ **(a$_2$)** Bouguer gravity anomalies were derived from satellite gravity data for profile L$_2$ **(a$_3$)** Near-surface representation lithostratigraphic section along the same baseline as the 2D model was deduced from satellite gravity data (a$_4$) Interpretation of the 2D model observations of the aforementioned magnetic and satellite gravity data.

Modeling of two-dimensional gravity and magnetic in profiles L$_4$ and L$_6$

The boundary patterns within the Formation were revealed by 2D forward modeling of some selected profiles (L$_4$ and L$_6$) over the Paleocene sediments of Sokoto Group, the Maastrichtian sediments of Rima Group, and the pre-Maastrichtian sediments of Gundumi and Illo Formations (Fig. 8). This was used in conjunction with satellite gravity anomalies and geologic interpretation of the reported aeromagnetic signals to determine the general basin architecture in the research area. In the 2D models, the Maastrichtian sediments of Rima Group were given a magnetic susceptibility value of 1.2013E-05 SI, whereas the Paleocene sediments of Sokoto Group were given 1.303E-03 SI. Using a magnetic susceptibility of 1.050E-03 SI and altering the basement depth between ~16.5 to ~28.9 km, different magnetic expressions of the basin configuration were taken into account. Two large depressions were visible in the subterranean basement relief, separated by a horst of Gundumi Formation that represented a horst of Illo Formation and sub-basin architecture (Abdulganiyu, 2021; Kogbe, 1979; Obaje, 2009). The basin sedimentary thickness, which ranges from ~3.5 km to more than ~5 km, indicates that these areas are very promising for hydrocarbons (Obaje et al. 2013; Adamu et al. 2022). Reduced to magnetic equator anomaly map observe of fluctuating high and low aeromagnetic signals. Additionally, high magnetic anomalies point to areas that are rich in magnetite (intrusive bodies).while regions with low magnetic anomaly show areas with relatively low content. The block structure and ridged morphology of the basement rocks below are reflected in these variations. The interpreted high and low magnetic responses point to a high susceptibility basement uplift and low susceptibility sediment filling depression, which imposes a rock architecture on the basin's underlying basement rocks. A magnetic depth to basement analysis has revealed that the basement surface is generally intermediate, and attain a maximum depth of 14. 20 km at the extreme ENW corner of the basin. The regional dip is gentle, and measured 0.5 in the east-western direction. Two dimensional interpretation of the satellite gravity data led to the following conclusions: The isolated intrusive bodies around Yauri, Bagudo, Zuru, and Maru coalesce into one big pluton (schist belt), just beneath the ground surface and extend to a depth of ~10. 26 km with steeply dipping contacts which suggest a magmatic origin for the granite ore bodies. The sediments of the Paleocene of Sokoto and the Maastrichtian of Rima Groups (Fig. 8) are generally outward dipping, and attain a general thickness of ~4.79 to ~14.34 km (Table 3), terminating in a characteristic gently undulating plane. This simple structural style suggests that the sequence cover was probably affected by only one tectonic event which left a (N to S) trending structural grain on the said rock units. A number of depressions in the subsurface basement rocks have been revealed where lower and upper crust thicknesses range from ~6.48 and ~4.79 km. Over the basin, both satellite gravity and magnetic data have revealed an irregular basement floor resulting from gentle folding of the sub-basin depression along a general N to S axis (Fig. 2 a,b), at wavelength scales of roughly 100 km and amplitudes of only a few hundred meters (Kogbe, 1981). Several sediments filled troughs and depressions on the basement surface have been revealed which form targets for groundwater exploration. The absence of major faulting even at the sediment - basement boundary tend to suggest that this southeastern sector of the Iullemmeden Basin probably originated from gentle epeirogenic warping's in contrast to the western and northeastern parts of the Niger Republic (Kogbe, 1981).

Science World Journal Vol. 18(No 4) 2023
www.scienceworldjournal.org
ISSN: 1597-6343 (Online), ISSN: 2756-391X (Print)
Published by Faculty of Science, Kaduna State University
DOI: https://dx.doi.org/10.4314/swj.v18i4.2

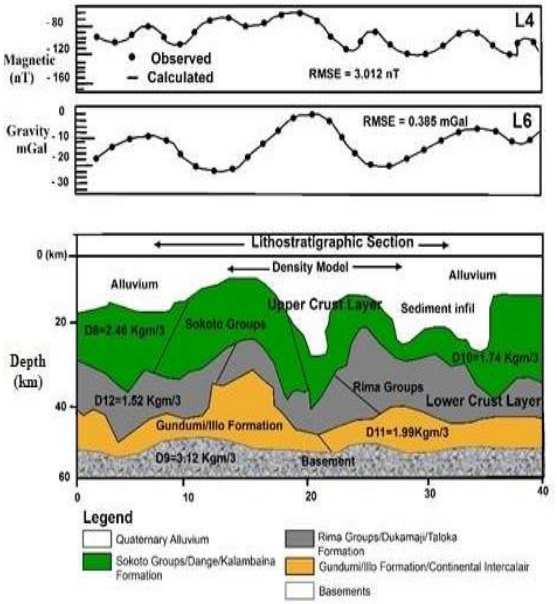

Figure 8: shows two-dimensional (2D) modeled profiles L_4 and L_6, magnetic and satellite gravity across the lithostratigraphic section of Quaternary alluvium, Sokoto and Rima Groups, the Gundumi and Illo Formation and the Basement complex of the study area. Using the program Gm-sys/Geosoft, the 2D modeling was carried out in a trial-and-error methodology while imposing some known geological and lithological restrictions (see the text for details). The units of density are in g/cm^3.

Conclusions

In this study, the utility of using satellite gravity data (Bouguer gravity anomalies of the WGM, 2012) and aeromagnetic data (RTE, anomalies) in imaging the deeply embedded crustal framework by focusing on the tectonic settings of the southeastern sector of Iullemmeden Basin were carried out. The deep-rooted Crustal framework or patterns of geological components, as determined from Bouguer gravity and reduce to magnetic equator, RTE anomaly maps, were updated and refined using the directed filtering analysis, edge detection, and depth to basement approach, this data is further analyzed utilizing upward continuation, derivative analysis, and two-dimensional gravity and magnetic modeling. Crustal features "limits" are clearly defined by the edge identification method for the potential field data under this study (such as satellite gravity and aeromagnetic). The regional Bouguer gravity anomaly, which is still trending northward, and the RTE anomaly reveal an E of W, NW of SE trend that is consistent with the Basin's overall trend. NE of SW trending lineaments can be seen in magnetic anomalies when the horizontal gradient of the tilt angle derivative (HGTD) is used. The findings of HGTD have led to the discovery of a number novel structural characteristics. The upper crustal level could be defined by a high-density intrusive body and sediment infill utilizing two-dimensional modeling that uses complete Bouguer gravity and reduced to magnetic equator. According to the results of the spectrum analysis of residual Bouguer gravity anomaly, the average estimated depth gauges for deep (Moho) and intermediate (Lower and upper crust) sources, respectively, are ~23.31 km and ~4.06 km, while that of reduce to equator, RTE anomaly, the average estimated depth are ~10.26 km and ~7.54 km, respectively.

Acknowledgement

The Federal University Birnin Kebbi administration, in conjunction with institutional based research proposal, IBR and the local Tertiary Education Trust Fund Intervention (Tetfund), Nigeria is gratefully acknowledged by the authors for providing financial support for the acquisition of the HRAM datasets and facilities made available during this research.

Data Availability

High-resolution aeromagnetic data can be purchased from the Nigeria Geological Survey Agency (NGSA) but is not publicly accessible. The US Geological Survey (USGS) website provides free access to the Satellite gravity data of the WGM, 2012, that were used for this investigation.

REFERENCES

Azer, M.K., (2013). Evolution and economic significance of listwaenites associated with Neoproterozoic ophiolites in South-Eastern Desert, Egypt. Geologica Acta 11 (1), 113–128.

Alexander, I., Samuel, O.O., Esther, C.M., Theophillus, T.E., Kingsley, C.I., Kingsley, C.N., (2015). Integrating Landsat-ETM and Aeromagnetic data for enhanced structural interpretation over Naragwata area, North-Central Nigeria. International Journal for Science and Engineering Research 6 (9), 2229–5518.

Araffa, S.A.S., Rabeh, T.T., Mousa, S.A.W., Abdel Nabi, S.H., Al, D.M., (2020). Integrated geophysical investigation for mapping of manganese-iron deposits at Wadi Al Sahu area, Sinai, Egypt—a case study. Arabian Journal of Geosciences 13, 823.

Abdulganiyu, Y., (2021). Stratigraphy and Sedimentology of Maastrichtian to Palaeocene Stratigraphic Succession of Gada Sheet4, Sokoto Sheet 10 and Rabah Sheet 11 South-western Sector of Iullemmeden (Sokoto) Basin Northwestern Nigeria. Unpublished Ph.D. thesis, Department of Geology, Ahmadu Bello University Zaria, Nigeria.

Adamu, A., Likkason, O.K. (2022). Exploring the Application of potential field Gravity Method in characterizing regional-trends of the Earth's sequence system over the Sokoto Basin, Northwestern Nigeria "in Earth Crust and its evolution from Pangea to the present continents. IntechOpen Ltd, DOI: http://doi.org/10.5772/intechopen.102940.

Adamu, A., Likkason, O.K., Maigari, A.S., Ali, S. and Agada, E.M. (2021a). Subsurface Investigation of geological structures from magnetic method in parts of Kangiwa, Gwandu formation, Northwestern Nigeria "6th International Conference on Engineering Geophysics (ICEG) Virtual, 25-28, October 2021. Al-Ain, UAE, 10.1190/iceg2021-085.1, pp. 336-341.

Adamu, A., Likkason, O.K., Maigari, A.S., Ali, S. and Ologe, O. (2020). Subsurface and lithological evidence from Aeromagnetic data in some parts of the Sokoto Basin, Northwestern Nigeria. Zimbabwe J.Sci.technol. Vol.15 (20), e-ISSN 2409-0360, pp. 116-127.

Adamu, A., Likkason, O.K., Maigari, A.S., and Ali, S. (2021b). Structural mapping insight from Gravity data for hydrocarbon accumulation in some parts of the Sokoto Basin, Northwestern Nigeria "in 7th Assembly of Arab

Conference on Astronomy and Geophysics (ACAG-7) Institute for Astronomy and Geophysics NRIAG, Cairo Egypt.

Bonde, D.S., Udensi, E.E., and Momoh, M., (2014). Modeling of Magnetic Anomaly zones in Sokoto Basin, Nigeria. IOSR Journal of Applied Geology and Geophysics, 2(1): 19-25.

Botros, N.S., 2014. Gold in Egypt: Does the future get worse or better? Ore Geology Reviews. 67, 189–207.https://doi.org/10.1016/j.oregeorev.2014.11.018.

Darly, M.C., Chorowitz, J. and Fairhead, J.D. (1989). The reactivation of steep basement shear zones and their influence on rift basin in Africa. Geological Society of London. **50**

Eldosouky, A.M., Abdelkareem, M., Elkhateeb, S.O., (2017). Integration of remote sensing and aeromagnetic data for mapping structural features and hydrothermal alteration zones in Wadi Allaqi area, South Eastern Desert of Egypt. Journal of African Earth Sciences 130, 28–37.

ElGalladi, A.A., Ghazala, H.H., Mansour, S.A., Gomaa, H.H., (2016). ''Integrated geophysical studies for mineral exploration at Wadi-Dendekan, Hamata area, South-Eastern Desert, Egypt." Annals of Geological Survey of Egypt, ISSN: 1110-0435, Vol. 33, PP.24.

Fairhead, J. D., and Okereke, C. S. (1988). A regional gravity study of the West African rift system in Nigeria and Cameroon and its tectonic interpretation. Tectonophysics, 143,141–159.

Gabr, S.S., Diab, H., Abdel Fattah, T.A., Sadek, M.F., Khalil, K.I., Youssef, M., (2022). Aeromagnetic and Landsat-8 data interpretation for structural and hydrothermal alteration mapping along the Central and Southern Eastern Desert boundary. Egypt. The Egyptian Journal of Remote Sensing and Space Science. 25, 11–20.https://doi.org/10.1016/j.ejrs.2021.12.002.

Ghazala, Hosni; Mebed, Mohamed; ElGalladi, Ahmed and Tawfiek, Hamada, (2016). ''Geophysical prospecting for locating probable areas of mineralization in WadiMeisah, southeastern desert, Egypt." Annals of Geological Survey of Egypt, ISSN: 1110-0435, Vol.33, PP-18.

Likkason, O.K., (2011). Spectral Analysis of Geophysical data-in Advances in Data, Methods, Model and their Applications in Geoscience: Intechopen. Doi: 10.5772/28070.

Likkason, O.K., Singh, G.P., and Samaila, N.K., (2013). A study of the Middle Benue Trough (Nigeria). Based on Geological Application and Analysis of Spectra of Aeromagnetic Data-in Energy sources part, Recovery Utiliztion and Environmental Effects. Doi: 10.1080/15567036.2010.514588.

Likkason, O.K., (2014). Exploring and Using the Magnetic Methods – in Advanced Geosciences and Remote Sensing, Intechopen, https://dx.doi.org/10.5772/57163.

Mekkawi, M.M., (2012). Application of Magnetic Method in Mineral Exploration: Iron-Ore Deposit, South Zagros Suture Zone. Egyptian Geophysical Society Journal. 10 (1), 117–124.

Mekkawi, M.M., El-Emam, A.E., Taha, A.I., Al Deep, M.A., Araffa, S.A.S., Massoud, U.S., Abbas, A.M., (2021). Integrated geophysical approach in exploration of iron ore deposits in the North-eastern Aswan-Egypt: a case study. Arabian Journal of Geosciences 14 (8).

Mousa, S.A., Abdel Nabi, S.H., Sultan, S.A., Mansour, S.A., Al-Deep, M.A., (2020). Geophysical exploration of titanomagnetite ore deposits by geomagnetic and geoelectric methods. SN Applied Sciences. 2, 444. https://doi.org/10.1007/ s42452-020-2206-5.

Nwankwo, Levi I., Shehu, Amada T., Evaluation of Curie-point depths, geothermal gradients and near-surface heat flow from high-resolution aeromagnetic (HRAM) data of the entire Sokoto Basin, Nigeria, Nigeria, Journal of Volcanology and Geothermal Research (2015), doi: 10.1016/j.jvolgeores.2015.09.017.

Jones, B. (1948). The sedimentary rocks of Sokoto province. Geological Survey Nigeria Bulletin 18: 1-75.

Kogbe, C.A. (1979). Geology of the Southeastern (Sokoto) Sector of the Iullemmeden Basin. Bulletin Geology Department, Ahmadu Bello University, Zaria, Nigeria 2:1, 42-64.

Kogbe, C.A. (1989). Cretaceous and Tertiary of the Iullemmeden Basin in Nigeria. In: C.A. Kogbe (eds.), Geology of Nigeria, 2nd edn, Rock View, Jos.

Obaje, N. G., Faruq, U.Z., Bomai, A., Moses, S.D., Ali, M., Adamu, S., Essien, A., Lamorde, U., Umar, M.U., Ozoji, T., Okonkwo, P., Adamu, L., and Nda, I.A. (2020). A Short Note on the Petroleum Potential of the Sokoto Basin in Northwestern Nigeria. Petroleum Science and Engineering. **4** (1), 34-38.

Obaje, N.G. (2009). Geology and mineral resources of Nigeria: Lecture Notes in Earth Sciences, Springer, Berlin Heidelberg.

Obaje, N.G., Aduku, M., and Yusuf, I. (2013). The Sokoto Basin of northwestern Nigeria: a preliminary assessment of hydrocarbon prospectivity, Petroleum Technology Development Journal 3 (2), 66-80.

Ramadan. T.M., Abdelsalam. M.G, and Stem. R.J., (2001). "Mapping Gold-Bearing Massive Sulfide Deposits in the Neoproterozoic Allaqi Suture, Southeast Egypt with Landsat TM and SIR=C/X SAR Images". Photogrammetric Engineering & Remote Sensing Vol. 67, No. 4, April 2001, pp. 491-497.

Reid, A.B., Allsop, J.M., Ganger, H., Millett, A.J., Somerton, I.W., (1990). Magnetic interpretation in three dimensions using Euler deconvolution. Geophysics 55 (1), 80–91.https://doi.org/10.1190/1.1442774.

Salem, A., Williams, S., Fairhead, J.D., Ravat, D., Smith, R., (2007). Tilt-depth method: A simple depth estimation method using first-order magnetic derivatives. The Leading Edge 26 (12), 1502–1505.https://doi.org/10.1190/1.2821934.

Salem, S.M., Arafa, S.A., Ramadan, T.M., El-Gammal, E.A., (2011). Exploration of copper deposits in Wadi-ElRegeita area, Southern Sinai, Egypt, with contribution of remote sensing and geophysical data. Arabian Journal of Geosciences 6 (2), 321–335.https://doi.org/10.1007/s12517-011-0346-z.

Spector, A., Grant, F.S., (1970). Statistical Models for Interpreting Aeromagnetic Data. Geophysics 35 (2), 293–302.https://doi.org/10.1190/1.1440092.

Sultan, S.A., Mansour, S.A., Santos, F.M., Helaly, A.S., (2009). Geophysical exploration for gold and associated minerals, case study: Wadi-El-Beida area, South-Eastern Desert. Egypt. Journal of Geophysics and Engineering 6 (4), 345–356. https://doi.org/10.1088/1742-2132/6/4/002.

Udoh, E.E. (1995). Modellierung der Grundwasserströmung im Sokoto-Becken, Nigeria. Shaker, Aachen.

Udoh, R.K. (1970). Geographical regions of Nigeria, Heinemann, London.

Wright, J.B., D.A. Hastings, W.B. Jones, and H.R. Williams. (1985). Geology and mineral resources of Africa.George Allen & Urwin, London..